Effect of Non-Markovian Collisions on Measured Integrated Line Shapes of CO

Zachary D. Reed,[1,*] Ha Tran,[2] Hoa N. Ngo,[3] Jean-Michel Hartmann,[2] and Joseph T. Hodges[1]
[1]Chemical Sciences Division, National Institute of Standards and Technology, Gaithersburg, Maryland 20899, USA
[2]Laboratoire de Météorologie Dynamique/IPSL, CNRS, Sorbonne Université, Ecole Polytechnique, Institut polytechnique de Paris, Ecole Normale Supérieure, PSL Research University, 4 place Jussieu, 75252, Paris, France
[3]Faculty of Physics, Hanoi National University of Education, 136 Xuan Thuy, Cau Giay, Hanoi, Vietnam

(Received 15 September 2022; revised 25 January 2023; accepted 10 March 2023; published 4 April 2023)

Using cavity ring-down spectroscopy to probe R-branch transitions of CO in N_2, we show that the spectral core of the line shapes associated with the first few rotational quantum numbers, J, can be accurately modeled using a sophisticated line profile, *provided* that a pressure-dependent line area is introduced. This correction vanishes as J increases and is always negligible in CO-He mixtures. The results are supported by molecular dynamics simulations attributing the effect to non-Markovian behavior of collisions at short times. This work has large implications because corrections must be considered for accurate determinations of integrated line intensities, and for spectroscopic databases and radiative transfer codes used for climate predictions and remote sensing.

DOI: 10.1103/PhysRevLett.130.143001

The dipole moment surface of a molecule plays an important role in chemical physics since its knowledge provides information about the molecular structure and internal dynamics. Furthermore, because the dipole moment matrix element, $\vec{\mu}_{if}$, for an optical transition between the molecular internal levels i and f couples radiation and matter, it contributes to light absorption and emission and, consequently, to radiative transfer in gas media and its various applications. The so-called integrated line intensity, S_{if}, is a key quantity for two reasons. First, because S_{if} is theoretically proportional to $|\vec{\mu}_{if}|^2$, its measurement enables testing of *ab initio* computed dipole moment surfaces. Second, S_{if} values are, together with the associated line positions and shapes, needed for modeling absorption spectra used in numerous applications. This explains why considerable efforts have been devoted to their measurement and prediction for over fifty years. This research has enabled steady progress (e.g., [1]) in the expansion of spectroscopic databases (e.g., [2–5]).

It is important to distinguish between the theoretical line intensity of a transition, S_{if}, and its experimental counterpart, the integrated fitted line shape, ILS_{if}, which is the area per absorber number density obtained from the analysis of measured spectra. The former, which depends only on i, f, and temperature, can be determined quantum mechanically without reference to collisional processes that influence the line shape. In contrast, the latter is an experimentally derived quantity, usually obtained by fitting a parametrized line profile to a measurement of the absorption coefficient, $\alpha(\nu)$, where ν is the optical frequency. Given this distinction, any deviation between the assumed and true line profiles can result in an ILS_{if} that does not equal the theoretical line intensity, S_{if}.

For ILS_{if} determinations, as well as for the other spectroscopic parameters and models involved in calculations of spectra of molecular gases, the accuracy requirements have considerably increased in the last decades for two main reasons. The first is that *ab initio* calculations of line intensities (e.g., [6–10]) and individual line shapes (e.g., [11–14]) now achieve accuracies at the few 0.1% level, implying that the measurements used to validate them should have a comparable uncertainty. The second is that the detection of sinks and sources of greenhouse gases from space observations requires absorber retrievals from atmospheric transmission spectra, and thus also calculated light-matter interactions, at a level of typically 0.2% (see, e.g., [15,16]). Achieving such low uncertainties in measurements of ILS_{if}s (and line shapes) is now possible (e.g., [17–21]).

For an isolated optical transition, models of measured and predicted spectra are described by $\alpha_{if}d\nu$, and are usually obtained by interchanging ILS_{if} with S_{if} in the expression

$$\alpha_{if}(\nu)d\nu = n_a c \mathrm{ILS}_{if} \Phi_{if}(\nu)d\nu, \tag{1}$$

where n_a is the absorber number density, c is the speed of light, and $\Phi_{if}(\nu)$ is the pressure-, temperature-, and mixture-composition-dependent assumed line profile normalized to unit area upon integration over frequency. The ILS_{if} (typically assigned to be the measured S_{if}), and

usually other line-profile parameters, are generally obtained by least-squares fits of the model on the right-hand side of this equation to a measured spectrum $\alpha_{if}(\nu)$ for a known n_a. Thus, consistent with the theoretical $S_{if}(T)$, the ILS_{if} is assumed to be independent of the gas sample composition and pressure. It is clear that $\Phi_{if}(\nu)$ also serves to extrapolate the data to spectral detunings beyond the measurement range, and that the fitted value of ILS_{if} will be sensitive to imperfections in the assumed far-wing behavior of $\Phi_{if}(\nu)$. Indeed, it was shown that the pressure independence of ILS_{if} breaks down when narrow intervals around rare-gas broadened lines of HF [22], HCl [23], and HI [24] are fit using Lorentzian profiles. The observed decreases of ILS_{if}s with the gas density were attributed [23,25,26] to the inadequacy of the Lorentz shape resulting from the breakdown of the impact approximation due to non-Markovian collisions, and, to a lesser extent, to the formation of molecular complexes [22,23]. However, the potential for similar effects in the case of molecules of more practical interest has not been investigated so far. The reasons for this are likely twofold. First, the observed decreases of ILS_{if}s with pressure were small (typically below 10% MPa^{-1}) so that their quantification required that measurements be made at high pressures (up to several MPa). For such conditions, only the above-mentioned hydrogen halides have rotational constants large enough to ensure that the lines are well spaced. Second, for molecules with more closely spaced transitions, measurements must be made at significantly lower pressures, which requires experimental accuracies that have only recently become available.

Here, we experimentally and theoretically demonstrate that the decrease of the measured ILS_{if} with pressure is a generic phenomenon caused by the use of improper collision-driven line profiles. To show this effect, accurate and precise comb-locked cavity ring-down spectroscopy absorption measurements were made for rovibrational lines of $^{12}\mathrm{C}^{16}\mathrm{O}$. These spectra presented were acquired using the rapid scanning technique given in [27] with the spectrometer and Cs-clock referenced laser configuration described in [28] (see Supplemental Material [29] for more details). This setup yields absorption coefficients with extremely high precision and signal-to-noise ratio, providing peak areas with relative standard uncertainties at the 0.1% level (absolute accuracy) [10].

All data were acquired on binary mixtures of CO diluted in N_2 or He at room temperature, T, over total pressure, p, ranging from 10 to 133 kPa. Measurements were made of the R1, R3, R5, and R7 (3-0) band transitions for CO-N_2 mixtures, and only the R1 transition for CO-He mixtures. We computed the CO number density as $n_a = x_{\mathrm{CO}} n_i(T,p)/Z(T,p)$ where x_{CO} is the CO mole fraction, n_i is the ideal-gas number density, and $Z(T,p)$ is the compressibility factor of the mixture accounting for real-gas behavior. For both CO-N_2 and CO-He mixtures this factor was evaluated over the experimental range of p, T, and x_{CO} using [30].

The ILS_{if}s were obtained by fitting the measured spectra using Eq. (1) and, for $\Phi_{if}(\nu)$, the eight-parameter Hartmann-Tran profile (HTP) [31] was used. Because some spectra showed slight evidence of line mixing [32], we modeled this perturbation using first-order theory [33], which improved the fits but with negligible changes in measured peak areas. The model also included a linear baseline and contributions from the wings of the nearest two (3–0) band CO lines. Examples of the high quality of spectra and further details of the HTP fitting may be found in the Supplemental Material [29].

All runs for a given line were combined and analyzed using a weighted least-squares linear fit of the measured ILS_{if}s as a function of pressure p. This approach yielded the intercept, $\mathrm{ILS}_{if}(p=0) \equiv S_{if}^{(\mathrm{exp})}$, and relative intensity-correction slope, $a_{if} = -[d\mathrm{ILS}_{if}(p)/dp]/\mathrm{ILS}_{if}(p=0)$. Figure 1 summarizes these results with each y axis

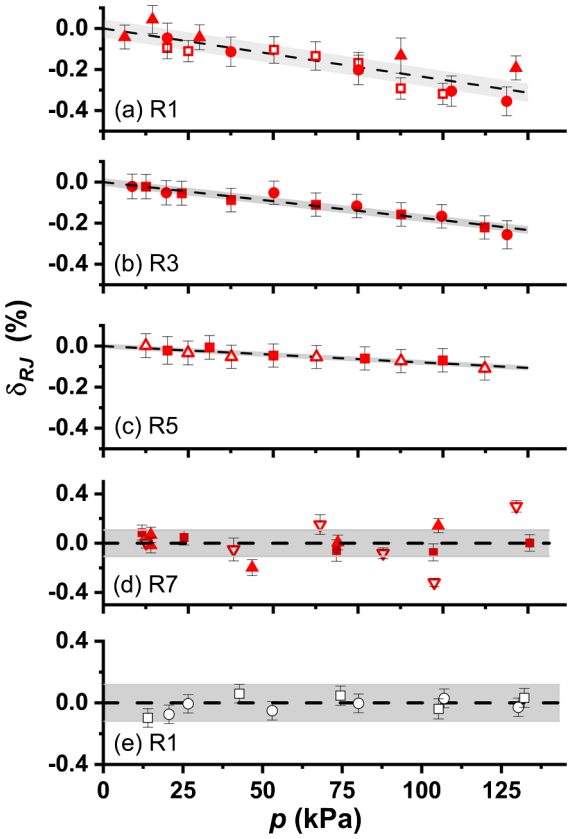

FIG. 1. Pressure dependence of the relative differences in the integrated line shapes for (3-0) band R-branch transitions of CO, where $\delta_{\mathrm{RJ}} = \mathrm{ILS}_{\mathrm{RJ}}(p)/\mathrm{ILS}_{\mathrm{RJ}}(p=0) - 1$, where RJ specifies the $i \to f$ transition. Cases shown are CO-N_2 [red symbols, panels (a)–(d)] and CO-He [black open symbols, panel (e)] corresponding to the indicated R-branch J lines. Solid lines are linear least-squares fits to the data and the gray regions encompass $\pm 1\sigma$ uncertainty in the fit. The various symbols for each case correspond to different samples.

corresponding to the relative difference $\delta_{if} = \mathrm{ILS}_{if}(p)/\mathrm{ILS}_{if}(p=0) - 1$ (i.e., $-a_{if}p$ in the fit). For each transition, δ_{if} is independent of our assigned $^{12}C^{16}O$ mole fraction provided that the actual value remains constant from sample to sample and as pressure changes. Figure 1 demonstrates the high consistency of the evolution of the retrieved ILS_{if}s with pressure. The indicated J values in this figure represent the rotational quantum number for transitions in the R-branch ($\Delta J = 1$). The intensity-correction slopes, a_{if}, are [2.9(3), 1.7(2), and 0.8(1)]% MPa^{-1} for the R1, R3, and R5 lines of CO in N_2, respectively, while they are 0% (within the measurement precision) for the R7 line as well as for the R1 line measured in CO-He. We note that for the CO-N_2 data, not accounting for deviations from ideal-gas behavior would have caused a measurable reduction in the magnitudes of the resulting a_{if} values. In the case of the R5 line, the slope obtained assuming ideal-gas densities was 25% smaller than that recovered assuming real-gas densities, which is a change that is greater than the relative uncertainty in a_{if}. This example illustrates the need to include $Z(T, p)$ in the data analysis.

To explain the observed changes in measured ILS_{if}s with pressure, classical molecular dynamics simulations (CMDS) were carried out using the equations in Chap. 3 of [34] for CO-N_2 and CO-He at 296 K and 0, 101.3 kPa and 202.6 kPa. The molecules were treated as rigid rotors, with CO-N_2 and CO-He interactions described by site-site functional forms with Coulombic (for CO-N_2) and atom-atom contributions [35,36]. Requantization of the classical rotation of the CO molecules was implemented, as described in [25,37], and the spectra were calculated from the dipole autocorrelation function to yield the absorption coefficient [32]. The peak areas were then retrieved from the calculated spectra through fits using the HTP, as was done for the measurements. Note that this approach, for which more details are provided in the Supplemental Material [29], used no adjusted parameters.

Figure 2 shows the comparisons between the intensity-correction slopes determined from the measured (a_{if}) and CMDS-calculated (denoted by a_J and defined below) spectra, where the error bars correspond to the statistical uncertainties obtained from the linear fits (see Fig. 1). These results call for several remarks. First, the measurements and calculations for CO in N_2 consistently provide significant evidence of pressure-induced reduction of ILS_{if} for the first few R-branch lines as well as a decrease of the pressure effects with increasing J. However note that, with the exception of $J = 1$ for which the agreement between theory and experiment is good, calculations overestimate the magnitude of a_{if} and predict a too slow decay with J. Second, for CO-He, no decrease of the ILS_{if}s with pressure is predicted regardless of J, which is consistent with the observation for the R1 line. Also, assuming (based on the

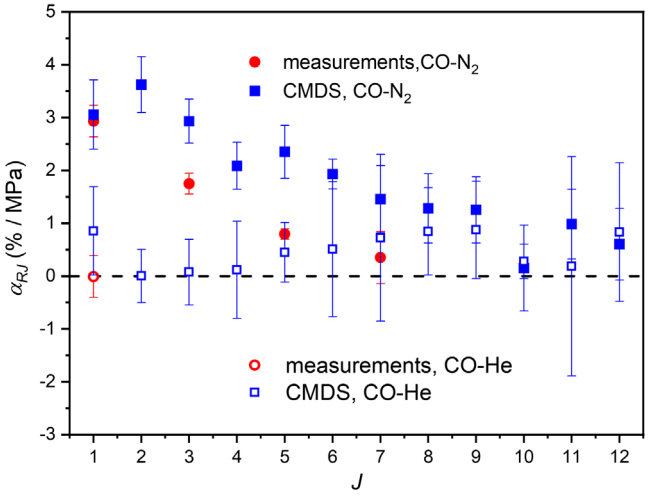

FIG. 2. Intensity-correction slopes obtained from measured (circles) and computed (squares) spectra versus the lower-state rotational quantum number J for RJ lines for CO-N_2 (full symbols) and CO-He (open symbols).

CO-N_2 results) that the measured slopes for CO-He decrease with J implies that negligible effects for this latter system would be observed for all lines.

To explain these results, we computed the time evolution of the relative number of molecules having the rotational quantum number J at time $t_0 = 0$ and remaining at this level at time t. The results in Fig. 3 show that, for CO-He and a given J value, the population closely follows the exponential decay, characteristic of Markovian behavior, over the entire time interval. In contrast, for CO-N_2, this occurs only after about 0.5 ps, the population decaying being significantly faster at earlier times. Note that both the amplitude of this non-Markovian behavior and the time interval over which it extends decrease with J. These findings can be explained by differences in the contribution of those collisions that are ongoing at t_0. Indeed, let us consider, for a given CO orientation, the CO-X potential

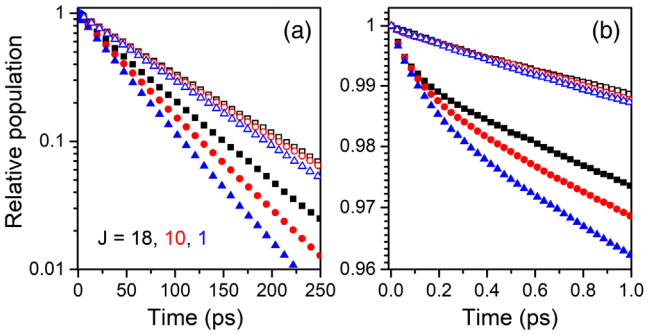

FIG. 3. Computed (see text) populations, normalized to unity at $t_0 = 0$, for CO diluted in N_2 (full symbols) and He (open symbols) at 296 K and 101.3 kPa (1 atm) for three rotational quantum numbers J shown over extended (a) and reduced (b) timescales.

$V(R)$ versus the intermolecular distance R. For CO-N_2, the repulsive fronts [where, e.g., $V(R)/k_B = 300$ K in which k_B is the Boltzmann constant] are at distances $R_{\min}$ ranging from 0.33 to 0.37 nm, while the attractive part vanishes [where, e.g., $V(R)/k_B = -20$ K] for $R_{\max}$ from 0.55 to 0.62 nm. For CO-He, $R_{\min}$ and $R_{\max}$ vary from 0.255 to 0.310 nm and from 0.390 to 0.415 nm, respectively. The relative numbers of molecules experiencing a collision at t_0 correspond to those having a partner between the two spheres of radii $R_{\min}$ and $R_{\max}$. For CO-N_2 at atmospheric density conditions corresponding to 296 K and 101.3 kPa, this number is $\simeq$0.0195, five times larger than the corresponding one for CO-He ($\simeq$0.0038). Furthermore, with mean relative speeds $v_r = 819$ ms^{-1} for CO-N_2 and 1338 ms^{-1} for CO-He, the effect of these collisions are typically $(R_{\max} - R_{\min})/v_r$ long, i.e., 0.3 ps and 0.1 ps for CO-N_2 and CO-He, respectively. These numbers explain why non-Markovian effects are observed at early times for CO-N_2 but not for CO-He.

Before returning to the results in Fig. 2, note that Fig. 4(a) shows that the time evolution of the population $\rho_J(t)$ can be modeled for pressure p by

$$\rho_J(t)/\rho_J(t_0 = 0) = (1 - a_J p)e^{-b_J p t} + a_J p e^{-c_J t}. \quad (2)$$

In this equation, $(1 - a_J p)$ and $b_J p$ are respectively the amplitude at $t_0 = 0$ and the rate of decrease of the Markovian exponential at long delays, while $a_J p e^{-c_J t}$ describes the non-Markovian behavior at early times. Now, if we neglect the influence of line mixing and the contribution of dephasing collisions to the decay of the dipole autocorrelation function, the spectrum of line J is directly obtained from the Fourier transform (FT) in time of $\rho_J(t)$ [25,32]. From Eq. (2), it is clear that the spectrum includes a narrow Lorentzian peak, of area $\rho_J(t = 0)(1 - a_J p)$ and HWHM in wave-number dimensions $b_J p/(2\pi c)$. [Note that, for $J = 1$, the value $(b_J p_0)^{-1} = 74.6$ ps at $p_0 = 101.3$ kPa from Fig. 4(a) leads to a pressure broadening coefficient of 0.701 cm^{-1} MPa^{-1} in good agreement with our measured HWHM of 0.767(2) cm^{-1} MPa^{-1}.] This part of the spectrum, associated with the FT of the first term in Eq. (2), is carried by a much weaker and broader Lorentzian [HWHM equal to $c_J/(2\pi c) \approx 38$ cm^{-1} for $J = 1$), of area $\rho_J(t = 0)a_J p$, resulting from the FT of $a_J p e^{-c_J t}$, as confirmed by Fig. 4(b). These elements qualitatively explain all the results in Fig. 2. Indeed, Fig. 3 indicates that for CO-He, no decrease of the ILS_{if} with pressure is observed since $a_J \simeq 0$, which is not the case for CO in N_2. Furthermore, the results for CO-N_2 in Fig. 4(a) confirm, although the effect is underestimated, that the intensity-correction slope a_J decreases with increasing J. Note that this is expected because stronger and stronger collisions are required to change the ρ_J population as the rotational speed (and J) increases.

Let us now discuss the measured integrated intensities $S_{if}^{(\mathrm{exp})}$ and use, for this purpose, the extremely accurate *ab initio* predictions of [10] as a reference. The values of $S_{if}^{(\mathrm{exp})} = \mathrm{ILS}_{if}^{(\mathrm{exp})}(p = 0)$ retrieved in this Letter, as well as the average values of $\mathrm{ILS}_{if}^{(\mathrm{exp})}(p)$ based on our measurements made near atmospheric pressure can be compared to the theoretical $S_{if}^{(\mathrm{theo})}$ in Fig. 5. As can be seen, the former measurements agree with $S_{if}^{(\mathrm{theo})}$ at the 0.5‰ level, which is within the present experimental uncertainty. For the $J = 1$, 3, and 5 transitions, ignoring the pressure effect and assuming $S_{if} = \mathrm{ILS}_{if}^{(\mathrm{exp})}(p \simeq 100$ kPa) results in

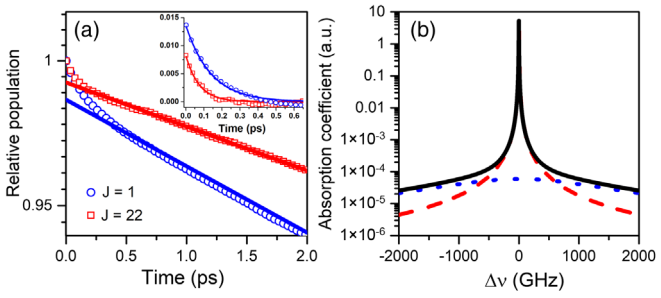

FIG. 4. (a) Exponential decay functions (lines) obtained from fits, at long time delays, of the relative populations (symbols) computed for $J = 1$ and $J = 22$ at 296 K and 101.3 kPa. The insert shows the differences between the latter and the former as well as their exponential fits. (b) The line spectrum for $J = 1$ (full line) calculated as the Fourier-Laplace transform of the relative population $\rho_{J=1}(t)$. The dashed and dotted lines represent the narrow and broad contributions associated respectively with the long- and short-time exponential decays of the populations.

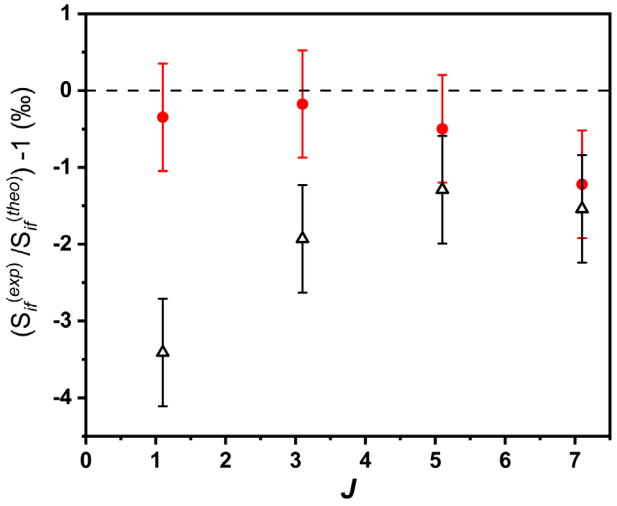

FIG. 5. Comparison between experimentally determined line intensities of CO RJ lines, $S_{if}^{(\mathrm{exp})}$, and *ab initio* values [10], $S_{if}^{(\mathrm{theo})}$. Closed red circles correspond to our data corrected with the experimental a_{if} values and open triangles correspond to our uncorrected results for pressures near 100 kPa.

deviations of 3.3‰, 1.9‰, and 1.3‰ relative to $S_{if}^{(\mathrm{theo})}$, respectively. These uncorrected values are well outside the measurement uncertainties, which brings an independent validation of the findings of the present study.

Thanks to precise and accurate comb-locked cavity ring-down spectroscopy measurements of CO transitions, we demonstrated that the integrated line shape $\mathrm{ILS}_{if}(p)$ obtained by fitting a standard profile to a measured spectrum in the core region of an absorption line if may decrease with the pressure p. To account for this effect, the pressure-independent theoretical line intensity, $S_{if} = \mathrm{ILS}_{if}(p = 0)$, must be multiplied by a factor $(1 - a_{if}p)$ to be consistent with measurements of $\mathrm{ILS}_{if}(p)$. This correction, which reduces the ILS_{if}s of CO in N_2 by about 0.3% at atmospheric pressure for the first few RJ lines, decreases quickly as J increases while it is always negligible for CO in He. These findings are well supported by molecular dynamics simulations that enable their attribution to the breakdown of the Markov (impact) approximation. We indeed show that the collisions ongoing at time zero transfer intensity from the core region of the line and thus reduce its area by shifting a fraction of the latter into a broad and weak continuum.

These findings should have numerous consequences. The first is that the phenomenon pointed out in this Letter must be taken into account in measurements of line intensities, particularly if a high accuracy is desired, when the experiments are made at pressures typically above 10 kPa. The second is that the computer codes used to calculate spectra need to be updated if they are used for applications such as accurate amount of substance measurements [38], isotope partitioning [39], and remote sensing [40,41]. Last but not least, spectroscopic databases must be extended to provide the a_{if} intensity-correction slopes to users. Even when restricted to gases of primary practical importance, this is a formidable task because the a_{if}s not only depend on the considered molecule and transition but also on the temperature and gas composition. Further, although the decrease in magnitude of the intensity-correction effect with J occurs rapidly for CO, we expect that it will tend to persist for higher J lines as the rotational constant of the absorber decreases. Finally, our results open perspectives for future studies of the limits of the Markov approximation for intermolecular collision effects on absorption spectra. Indeed, thanks to their dependence on the considered if line, measurements of a_{if} provide much more detailed information to investigate the influence of non-Markovian collisions than do the far line- and band-wing regions, where many transitions simultaneously contribute, generally used for such studies (see Chap. V of [32]).

The work at NIST was supported by the NIST Greenhouse Gas and Climate Science Measurements Program.

*Corresponding author.
zachary.reed@nist.gov

[1] L. Rothman, Nat. Rev. Phys. **3**, 302 (2011).
[2] I. Gordon, L. Rothman, R. Hargreaves, R. Hashemi, E. Karlovets, F. Skinner, E. Conway, C. Hill, R. Kochanov, Y. Tan *et al.*, J. Quant. Spectrosc. Radiat. Transfer **277**, 107949 (2022).
[3] T. Delahaye, R. Armante, N. Scott, N. Jacquinet-Husson, A. Chédin, L. Crépeau, C. Crevoisier, V. Douet, A. Perrin, A. Barbe *et al.*, J. Mol. Spectrosc. **380**, 111510 (2021).
[4] L. Rothman, I. Gordon, R. Barber, H. Dothe, R. Gamache, A. Goldman, V. Perevalov, S. Tashkun, and J. Tennyson, J. Quant. Spectrosc. Radiat. Transfer **111**, 2139 (2010).
[5] J. Tennyson, S. N. Yurchenko, A. F. Al-Refaie, E. J. Barton, K. L. Chubb, P. A. Coles, S. Diamantopoulou, M. N. Gorman, C. Hill, A. Z. Lam *et al.*, J. Mol. Spectrosc. **327**, 73 (2016).
[6] I. I. Mizus, A. A. Kyuberis, N. F. Zobov, V. Y. Makhnev, O. L. Polyansky, and J. Tennyson, Phil. Trans. R. Soc. A **376**, 20170149 (2018).
[7] A. V. Nikitin, M. Rey, and V. G. Tyuterev, J. Quant. Spectrosc. Radiat. Transfer **200**, 90 (2017).
[8] O. L. Polyansky, K. Bielska, M. Ghysels, L. Lodi, N. F. Zobov, J. T. Hodges, and J. Tennyson, Phys. Rev. Lett. **114**, 243001 (2015).
[9] X. Huang, D. W. Schwenke, R. S. Freedman, and T. J. Lee, J. Quant. Spectrosc. Radiat. Transfer **203**, 224 (2017).
[10] K. Bielska, A. Kyuberis, Z. Reed, G. Li, A. Cygan, R. Ciuryło, E. Adkins, L. Lodi, N. Zobov, V. Ebert *et al.*, Phys. Rev. Lett. **129**, 043002 (2022).
[11] M. Słowiński, F. Thibault, Y. Tan, J. Wang, A.-W. Liu, S.-M. Hu, S. Kassi, A. Campargue, M. Konefał, H. Jóźwiak *et al.*, Phys. Rev. A **101**, 052705 (2020).
[12] E. Serov, N. Stolarczyk, D. Makarov, I. Vilkov, G. Golubiatnikov, A. Balashov, M. Koshelev, P. Wcisło, F. Thibault, and M. Tretyakov, J. Quant. Spectrosc. Radiat. Transfer **272**, 107807 (2021).
[13] J.-M. Hartmann, H. Tran, N. H. Ngo, X. Landsheere, P. Chelin, Y. Lu, A.-W. Liu, S.-M. Hu, L. Gianfrani, G. Casa *et al.*, Phys. Rev. A **87**, 013403 (2013).
[14] H. T. Nguyen, N. H. Ngo, and H. Tran, J. Chem. Phys. **149**, 224301 (2018).
[15] C. E. Miller, L. R. Brown, R. A. Toth, D. C. Benner, and V. M. Devi, C.R. Phys. **6**, 876 (2005).
[16] T. Delahaye, S. E. Maxwell, Z. D. Reed, H. Lin, J. T. Hodges, K. Sung, V. M. Devi, T. Warneke, P. Spietz, and H. Tran, J. Geophys. Res. (Atmos.) **121**, 7360 (2016).
[17] G. Casa, D. A. Parretta, A. Castrillo, R. Wehr, and L. Gianfrani, J. Chem. Phys. **127**, 084311 (2007).
[18] A. Cygan, D. Lisak, P. Morzyński, M. Bober, M. Zawada, E. Pazderski, and R. Ciuryło, Opt. Express **21**, 29744 (2013).
[19] E. Fasci, T. A. Odintsova, A. Castrillo, M. D. D. Vizia, A. Merlone, F. Bertiglia, L. Moretti, and L. Gianfrani, Phys. Rev. A **93**, 042513 (2016).
[20] A. J. Fleisher, E. M. Adkins, Z. D. Reed, H. Yi, D. A. Long, H. M. Fleurbaey, and J. T. Hodges, Phys. Rev. Lett. **123**, 043001 (2019).
[21] K. Bielska, A. Cygan, M. Konefał, G. Kowzan, M. Zaborowski, D. Charczun, S. Wójtewicz, P. Wcisło, P. Masłowski, R. Ciuryło *et al.*, Opt. Express **29**, 39449 (2021).

[22] A. Kouzov, K. Tokhadze, and S. Utkina, Eur. Phys. J. D **12**, 153 (2000).
[23] C. Boulet, P.-M. Flaud, and J.-M. Hartmann, J. Chem. Phys. **120**, 11053 (2004).
[24] M. O. Bulanin, A. Domanskaya, K. Kerl, and C. Maul, Mol. Phys. **104**, 2685 (2006).
[25] H. Tran, G. Li, V. Ebert, and J.-M. Hartmann, J. Chem. Phys. **146**, 194305 (2017).
[26] A. P. Kouzov, A. V. Sokolov, and N. N. Filippov, J. Quant. Spectrosc. Radiat. Transfer **278**, 108043 (2022).
[27] G. Truong, K. Douglass, S. Maxwell, R. van Zee, D. Plusquellic, J. Hodges, and D. Long, Nat. Photonics **7**, 532 (2013).
[28] Z. D. Reed, D. A. Long, H. Fleurbaey, and J. T. Hodges, Optica **7**, 1209 (2020).
[29] See Supplemental Material at http://link.aps.org/supplemental/10.1103/PhysRevLett.130.143001 for details of the experimental setup and the CMDS calculations.
[30] E. W. Lemmon, I. Bell, M. L. Huber, and M. O. McLinden, NIST Standard Reference Database 23: Reference Fluid Thermodynamic and Transport Properties-REFPROP, Version 10.0, National Institute of Standards and Technology (2018).
[31] J. Tennyson, P. F. Bernath, A. Campargue, A. G. Csaszar, L. Daumont, R. R. Gamache, J. T. Hodges, D. Lisak, O. V. Naumenko, L. S. Rothman *et al.*, Pure Appl. Chem. **86**, 1931 (2014).
[32] J.-M. Hartmann, C. Boulet, and D. Robert, *Collisional Effects on Molecular Spectra (Second Edition)* (Elsevier, Amsterdam, 2021).
[33] P. Rosenkranz, IEEE Trans. Antennas Propag. **23**, 498 (1975).
[34] M. Allen and D. J. Tildesley, *Computer Simulation of Liquids* (Oxford University Press, Oxford, 1987).
[35] J.-P. Bouanich, J. Quant. Spectrosc. Radiat. Transfer **47**, 243 (1992).
[36] A. B. Weaver and A. A. Alexeenko, J. Chem. Phys. Ref. Data **44**, 023103 (2015).
[37] H. Tran and J.-L. Domenech, J. Chem. Phys. **141**, 064313 (2014).
[38] J. A. Nwaboh, Z. Qu, O. Werhahn, and V. Ebert, Appl. Opt. **56**, E84 (2017).
[39] A. Fleisher, H. Yi, A. Srivastava, O. Polyansky, N. Zobov, and J. Hodges, Nat. Phys. **17**, 889 (2021).
[40] D. Crisp, R. Atlas, F.-M. Breon, L. Brown, J. Burrows, P. Ciais, B. Connor, S. Doney, I. Fung, D. Jacob *et al.*, Adv. Space Res. **34**, 700 (2004).
[41] G. Ehret, P. Bousquet, C. Pierangelo, M. A. Matthias, B. Millet, J. Abshire, H. Bovensmann, J. Burrows, F. Chevallier, P. Ciais *et al.*, Remote Sens. **9**, 1052 (2017).